Soft Matter

Accepted Manuscript

ROYAL SOCIETY OF CHEMISTRY

www.rsc.org/softmatter

Reversible Polypeptide Hydrogels from Asymmetric Telechelics with Temperature-dependent and Ni^{2+}-dependent Connectors.

Thao T. H. Pham, Jasper van der Gucht, J. Mieke Kleijn, Martien A. Cohen Stuart

Physical Chemistry and Soft Matter, Wageningen University,

Dreijenplein 6, 6703 HB Wageningen, The Netherlands

Correspondent email: Martien.CohenStuart@wur.nl

Abstract

An asymmetric ('hybrid') triblock polypeptide TR_4H with two different, orthogonally self-assembling end blocks has been constructed by conjugating a long (37 kDa) random coil block (R_4) with a triple helix former T = $(Pro\text{-}Gly\text{-}Pro)_9$ at the N terminus, and a histidine hexamer ('Histag', H) at the C terminus. This molecule can form trimers at room temperature by assembly of the T blocks, which can in turn assemble upon addition of Ni^{2+}, by association of Ni complexes involving the H block. This results in reversible hydrogels with dual responsiveness. We have studied mechanical properties of these gels, and compared them to gels formed by the symmetric triblock TR_8T which is equivalent to a dimer of TR_4H, but can only form triple helix-based networks. We find that there is an optimum mole ratio for Ni^{2+} with respect to the polypeptide of about 1; gels are weaker at both lower and higher Ni^{2+} dose. At the optimum dose, the high-frequency storage modulus is in between the value expected for nickel-induced dimerization and trimerization of the H blocks. We also find that the gels relax on time scales of about 50 s, which is two orders of magnitude faster than for TR_8T gels, implying that relaxation is dominated by the dynamics of the Ni^{2+} complex.

Introduction

Triblock copolymers with self-assembling end blocks are prone to form (reversible) networks and gel-like materials. The majority of these is of the symmetric class A-C-A, where A is the assembling block, and C the soluble connector [1-5]. Often, the A blocks are just poorly soluble, so that they assemble in a micellar core-like domain; the classical example here is PEO with two end-attached alkyl groups [6, 7]. There are also other cases where the self-assembly is based on a more specific structure, e.g., the formation of secondary structure such as a triple helix [8-10]. All these systems feature interesting mechanical behaviour, but are also simple in the sense that their self-assembling behaviour depends on a single chemical entity.

A smaller, but more intriguing class is that of asymmetric triblocks A-C-B, where A and B are orthogonal self-assembling blocks. For these latter systems, network formation can be influenced along different kinetic pathways, depending on the order in which the blocks A and B are triggered to assemble or disassemble, and short loops are excluded due to the orthogonality. We have shown that such systems can indeed form networks with path-dependent properties, because structural relaxation is often (very) slow [11, 12].

An orthogonal pair is conveniently obtained, e.g., when A has temperature-dependent solubility, while B undergoes electrostatically driven binding, *i.e.*, an interaction involving ions [13-15]. Constructing such triblocks with well-defined architecture by way of standard polymerization techniques is possible, but often cumbersome, because controlled 'living' polymerizations are required [16-19]. An alternative that is gaining popularity is to construct triblock copolymers exclusively from (natural) amino acids, and to use a biosynthetic approach, exploiting the genetic code to obtain the desired macromolecule [20]. This latter

approach has the added advantage that the polymers are biocompatible and biodegradable, providing a perspective for biomedical use. The present paper describes one such system; one of the end blocks is a triple helix-forming block denoted as T, which dissociates on heating; we have used this block before in symmetric triblocks TR_nT [8, 10], where R_n is the Random coil connector made up of *n* repeats of a hydrophilic random coil block [21]. For sufficiently high concentrations, TR_nT is known to form hydrogels at temperatures below 50 °C [8], due to the slow formation of T_3 (triple helical) nodes [9]. These gels become more rigid as temperature decreases. Eventually, when the fraction of T blocks in helices reaches 100% at temperature below 15 °C, the mechanical properties saturate; hence, the range of relevant temperatures for this block is between about 10 and 50 °C. The storage modulus reaches a maximum value depending on concentration, and on the length of the R_n block; typically, gels of TR_4T reach a storage modulus of about 500 Pa at 2 mM [8], whereas gels of TR_8T [10], in which the connector block is twice as long, reach that modulus at 1.2 mM.

The second self-assembling block is a hexahistidine block (H) which is known to assemble by complexation with divalent metal ions like, e.g., Zn^{2+} or Ni^{2+}, and is often referred to as 'Histag'[22, 23]. As far as we know, this latter kind of complexation has not been used in the context of self-assembling polypeptides. The purpose of this paper is to investigate how the triblock TR_4H assembles into a (hydro)gel and what the effect is of conditions on the mechanical properties of this gel, in particular as compared to TR_nT. Nickel-Histag complexation has recently been used to make networks from four-arm PEG stars [23] carrying single histidine end groups. However, Histags usually consist of a sequence of six histidines (His_6) for optimum binding to stationary phases in chromatography[24, 25], and it is also known that these can indeed associate to dimers (His6)2 and possibly also multimers $(His_6)_n$ when Ni^{2+} is added [22], and the pH is in an appropriate range (5 to 7). We therefore chose to use His_6 as the H block.

Experimental

Materials

The polypeptide studied in the present work, TR_4H, consists of three conjugated blocks: (i) the triple helix former T, which consists of nine repeats of the tripeptide Pro-Gly-Pro: $(PPG)_9$ [21], (ii) R_4, a tandem repeat of four highly hydrophilic, 9 kDa blocks which forms no secondary structure but only water-soluble random coils in a large range of pH and temperature, due to a quasi-random sequence with composition Gly:X:Y of 1:1:1; X and and Y are also hydrophilic amino acids, among which a significant fraction of proline; and (iii) H, a histidine hexamer.

The polymer was biosynthesized by *Pichia pastoris* strains which had been genetically modified to host the appropriate gene as a template. The construction of the gene has been described previously [26]. Briefly, the TR_4 gene [21] was digested with *Van91I* and then ligated with a double-stranded *DraIII/EcoRI* H block encoding the 6 Histidine residues. The resulted TR_4H gene was then cloned into *Pichia Pastoris* expression vector *pPIC9* (Invitrogen) for protein expression. The yeast was grown in a 2.5 L bioreactor as described previously[21]. Purification of the secreted protein, using ammonium sulfate at 40% saturation, was carried out as described before [21, 26]. The purified protein was dialyzed using 1 kDa Spectra/Por 7 tubing (Spectrum Labs) and freeze-dried for storage until use.

Methods

Dynamic light scattering (DLS)-based microrheology

Dynamic light scattering (DLS)-based microrheology was carried out in a Malvern Zetasizer at a wavelength (λ) of 544 nm and a scattering angle (ϑ) of 173°, corresponding to a scattering vector $q=4\pi/\lambda \sin\vartheta/2 \approx 0.02$ nm^{-1}. Carboxyl latex microspheres (Molecular Probes by Life Technologies) with a diameter of 400 nm were used as tracer particles. Prior to use, the

particles were diluted to a final weight to volume fraction of 0.1 % and sonicated to break up any agglomerates before mixing with the gelling samples. Similar latex microspheres had been used for multiple tracking micro-rheology on the symmetric TR_4T hydrogels, showing no undesired interaction between the tracers and the protein polymers [27]. The protein solutions were prepared in mixtures of 45 vol% 10 mM MES (2-(N-morpholino)ethanesulfonic acid) buffer and 55 vol% D_2O; this mixture was chosen to match the density of the tracer particles in order to minimize sedimentation. Solutions were prepared by dissolving protein at 50 ºC for at least 20 min to allow any triple helices in the sample to melt completely. Fresh $NiCl_2$ solution of 10 mM was added to the preheated protein solutions at different mole ratios in order to form coordination complexes between His_6 and the metal ion. The tracer particles were then introduced into the system at a final weight-to-volume fraction of 0.05 %, and mixed with the Ni/ TR_4H solution by vortexing. The samples with tracer particles were then introduced into a capped cuvette (Malvern) and incubated at 10 °C, allowing the formation of triple helices between the proteins. The viscoelastic behaviour of the Ni/ TR_4H system was then followed up to 20 hours. The microrheology measurements were done at protein concentrations slightly below the gelation point of the Ni/ TR_4H system, so that the displacement by Brownian motion is large enough to be observed. The changes in viscoelastic properties of the systems are indirectly calculated through the Brownian motion of the tracer particles [28], which is characterized by their mean-square displacement $\langle \Delta r^2(t) \rangle$. In the case of free diffusion, this is a linear function of time:

$$< \Delta r^2(t) >= 6Dt \quad (1)$$

Where D is the diffusion coefficient. For a spherical particle with hydrodynamic radius R in a solvent with viscosity η, the diffusion coefficient is given by the Stokes-Einstein relation:

$$D = \frac{kT}{\zeta} \quad (2)$$

Where *k*, *T* and ζ are the Boltzmann constant, temperature and Stokes' friction coefficient, respectively. Under no slip condition, the Stokes' friction coefficient is given as $\zeta = 6\pi\eta R$.

In our experiments, the concentration of the tracer particles (probes) was adjusted such that the scattered intensity of the probes was at least 20 times higher than that of the Ni/ TR_4H solutions alone, without particles. The contribution of the scattering of the Ni/ TR_4H matrix to the correlation function could be neglected. From the fluctuations in the scattered intensity we obtain the intensity correlation function defined as:

$$g^{(2)}(t) = \frac{<I(\tau)I(\tau+t)>}{<I(\tau)>^2} \quad (3)$$

In turn, the intensity correlation function is related to the normalized field autocorrelation function $g^{(1)}$:

$$g^{(2)}(\tau) = \beta\, g^{(1)\,2}(\tau) \quad (4)$$

where β is a proportionality factor and

$$g^{(1)}(t) = exp\left[-\frac{q^2}{6} < \Delta r^2(t) >\right] \quad (5)$$

Measurements performed at various scattering angles showed that the quantity

$q^{-2}ln[g^{(1)}(t)]$ is independent of the scattering vector [28]. Thus, all experiments in this study were performed at a fixed angle of 173 °.

Rheology

Rheological experiments were done with an Anton Paar MCR 501 rheometer equipped with C10/TI Couette geometry, with bob and cup diameter of 9.991 and 10.840 mm, respectively. The temperature was controlled by a Peltier system, which allows quick heating and cooling.

A solvent trap containing oil was used to minimize evaporation. The couette was preheated (50 °C) before adding sample solutions. After inserting the bob into the cup, the temperature was quickly lowered to 10 °C. Gel formation was monitored by applying a sinusoidal deformation to the system (frequency 1 Hz and amplitude 1 %). Viscoelastic dynamic analysis was performed in a frequency sweep range of 0.01-20 Hz with deformation amplitude of 1 %, well within the linear response range. Creep experiments were done at an applied stress of 2-10 Pa with duration of 1800 s. Freeze-dried protein was first dissolved in MES buffer and heated at 50 °C for at least 20 min to allow any triple helices in the sample to melt completely. Fresh Ni^{2+} solution of 10 mM was then added to the protein solutions and the mixture was kept at 50 °C for at least 10 mins to allow equilibration of the metal coordination between His_6 and Ni^{2+}.

Results and Discussion

Considering the results mentioned above for TR_nT triblocks, we decided to study TR_4H solutions quenched at 10 °C, at concentrations ranging from 0.75 mM to 1.75 mM, while varying the Ni^{2+}:TR_4H molar ratio (denoted as *f*) between zero and 2.0; we set the pH at 5.5 and 6.5, respectively, which is supposed to be the optimum condition for complex formation [22].

Samples were always prepared by dissolving TR_4H in 10 mM MES buffer at 50 °C, and then adding Ni^{2+}; under these conditions the H blocks can associate, but the T blocks do not form helices so that no gelation occurs (see supporting information fig. SI1). In a preliminary experiment, we compared gels at pH 5.5 and 6.5; it turned out (fig. SI2) that the strongest gels are obtained at pH 6.5. We therefore set the pH at 6.5 for all subsequent experiments.

After preparing the solutions, the temperature was quenched to 10 °C so that helices would form; the sample's mechanical properties were then characterized in various ways.

Our first set of experiments is done with 0.5 mM (20 g/L) TR_4H solution, to which varying amounts of Ni^{2+} are added to obtain f = 0, 0.25, 0.5, and 1.0. In fig. 1 we present DLS-based microrheology data taken 12 h after the quench. For comparison, we include the data for free tracer particles.

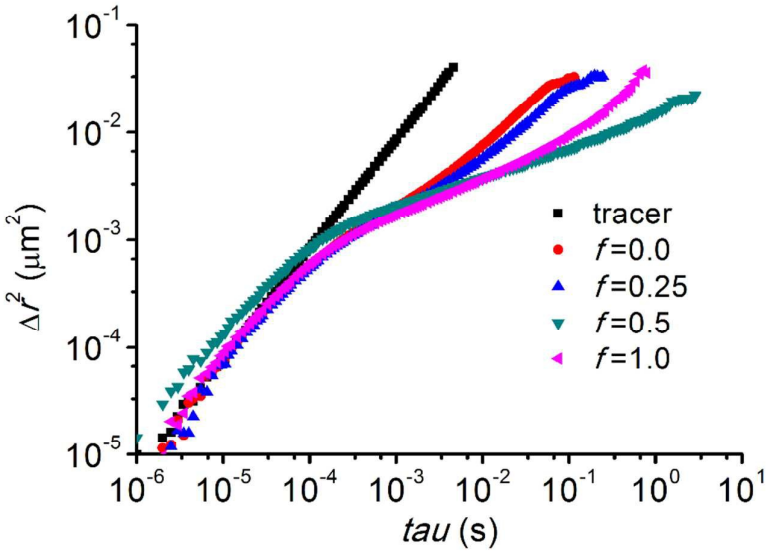

Fig. 1 Mean square displacement $<\Delta r^2>$ from dynamic light scattering) of probe particles in Ni/TR_4H system after 12 h at 10 °C at various Ni/TR_4H mole ratios. TR_4H concentration is of 20 g/L (0.5 mM).

As can be seen, free tracers (black) experience a simple Newtonian fluid: the mean square displacement Δr^2 (MSD) is diffusive over the entire time window probed. In other words, the correlation function is a simple exponential decay. In the presence of sufficient polymer, the diffusion of the particles is slowed down [28], and the decay is no longer a simple exponential. When the tracers are in a nickel-free TR_4H solution (red), we observed that the MSD becomes slightly subdiffusive at around 0.1 ms, signalling the formation of a weak network that hampers tracer diffusion. Upon adding Ni^{2+}, the subdiffusive behaviour is initially hardly

affected (blue, f = 0.25), but it becomes suddenly prominent at f = 0.5 (green), extending up to seconds in time; in this regime the mean square displacement follows a power law: $\langle \Delta r^2 \rangle \sim \tau^{0.28}$. Surprisingly, adding more Ni^{2+} (magenta, f = 1.0) restores diffusive behaviour beyond approximately 0.1 s, indicating a slight weakening of the network. Hence, it seems that in terms of network strength, there is an optimum Ni^{2+} dose.

This conclusion is confirmed by macroscopic rheology experiments carried out at higher TR_4H concentrations. In fig. 2A we plot, for a 1.25 mM sample, the storage modulus G' as a function of time after the quench.

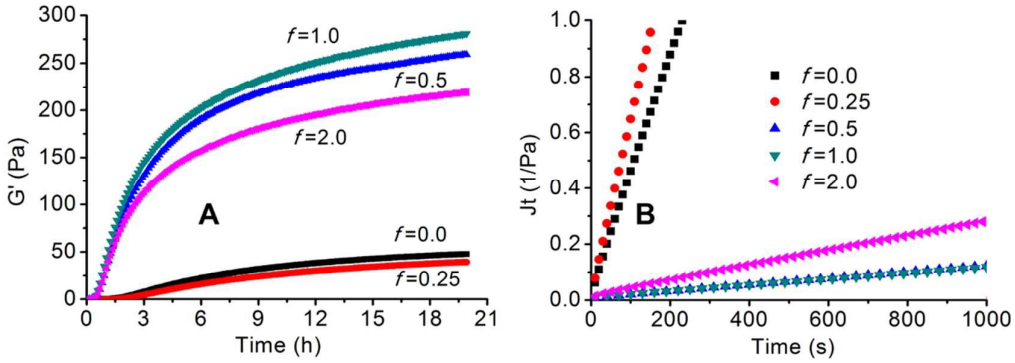

Fig. 2 (A) Storage modulus of Ni/TR_4H gels at 1.25 mM (50 g/L) protein concentration as a function of gelation time (after quenching to 10 °C) for various Ni/TR_4H ratios. (B) Creep compliance as a function of time for the same gels.

Without any Ni^{2+} (black), this systems slowly develops a small storage modulus (G') of 50 Pa over 20 h; upon adding Ni^{2+} at f = 0.25 (red) this remains the same. When the Ni^{2+} dose is doubled to f = 0.5 (blue), G' suddenly increases much more steeply, reaching a value of 250 Pa after 20 h. With a Ni^{2+} dose of f = 1.0 (green), the behaviour is very similar. Then, at f = 2.0 (magenta), the gel develops less strength, eventually reaching G' = 220 Pa.

Creep experiments (fig. 2B) yield a similar picture. The slope of the compliance (Jt) versus time plot, which probes the reciprocal of the effective low shear viscosity η, is high for f = 0

(black) and 0.25 (red), then drops to a low value for f = 0.5 and 1.0 (blue, green) , to recover somewhat for f = 2.0 (magenta).

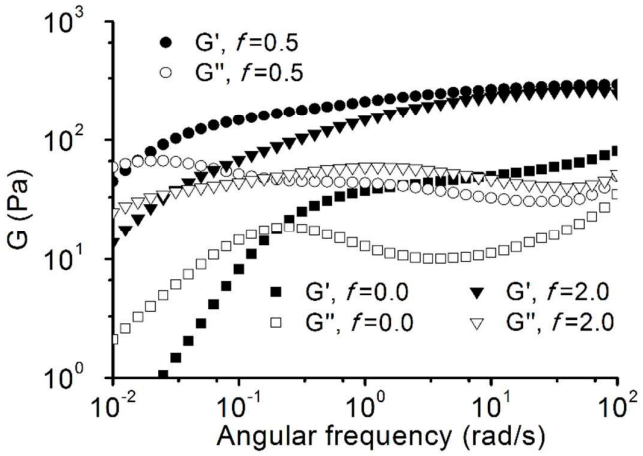

Fig. 3. Frequency dependence of storage modulus *G'* (closed symbols) and loss modulus *G''* (open symbols)for Ni/TR_4H gels at three different Ni^{2+} doses (0.0, 0.5 and 2.0).

The visco-elastic nature of the gelled system at 20 h is borne out in fig. 3 where storage modulus *G*' and loss modulus *G''* are plotted against frequency for a concentration of 1.25 mM and three different *f* values (0, 0.5, and 2.0). The nickel-free system is clearly visco-elastic, with a typical relaxation time of about 5 s, as deduced from the frequency where *G'*= *G''*. At f = 0.5, the relaxation time has gone up by about an order of magnitude (50 s), and both *G'* and *G''* are ten times higher. At f = 2.0, relaxation is somewhat faster again, and *G'* is clearly more frequency dependent than at f = 0.5, indicating a partial weakening of the gel.

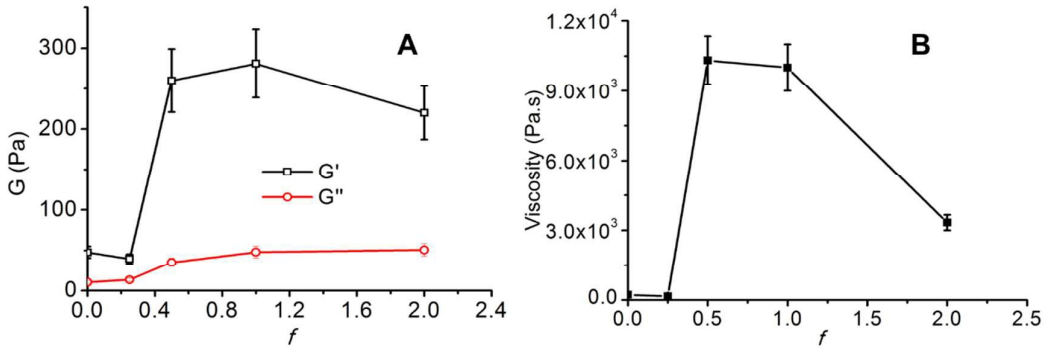

Fig. 4 Effect of Ni^{2+} dose on mechanical properties of Ni/TR_4H gels. (A) High-frequency moduli. (B) Zero-shear rate viscosity (from creep experiments).

We can summarize the data of fig. 2 by plotting, in fig. 4, *G'*, *G''*, and η as a function of f. As can be seen, Ni^{2+} has hardly any effect up to f = 0.25; then there is a strong increase in the elastic properties, followed by a broad maximum (f = 0.5 - 2.0). The low-shear viscosity clearly also peaks in the range f = 0.5 – 1.0 but the decay for higher Ni^{2+} dose is more prominent.

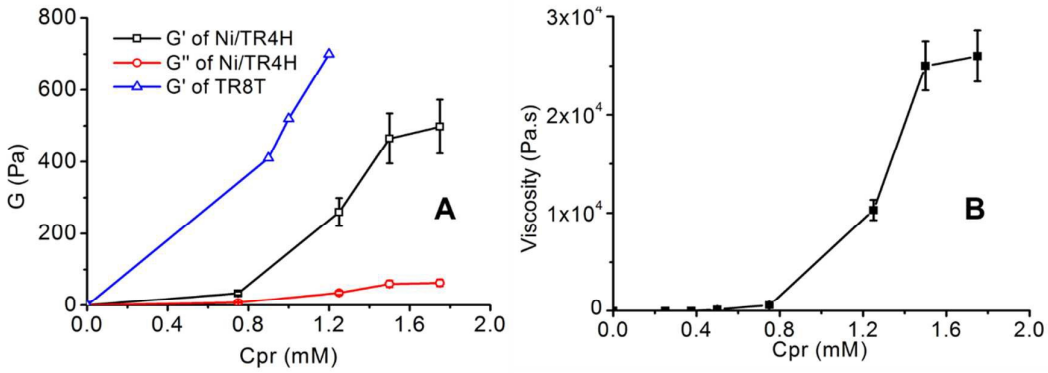

Fig. 5. Mechanical properties of Ni/TR_4H gels as a function of protein concentration, at fixed Ni:TR_4H molar ratio f = 1.0. (A) Storage (black) and loss (red) moduli. For comparison, storage moduli of a TR_8T gel from Teles et al. [10] are included (blue). (B) Zero-shear rate viscosity (from creep experiments).

The effect of protein concentration at a fixed Ni:TR_4H molar ratio f = 1.0 is summarized in fig. 5. Below a concentration of 0.8 mM, the gel is very weak, but beyond that threshold, its storage modulus G' increases rapidly, reaching values close 500 Pa. Qualitatively, it is clear that the system has responded to both temperature and added Ni^{2+} to form a transparent polymer gel (see fig. SI3) based on two kinds of reversible connections: triple helices and Ni_nHis_6 complexes which are both needed to form a sample spanning network. The Ni_nHis_6 complexes form the strongest gels at Ni:TR_4H ratios between 0.5 and 1.0; this suggests that the dominant species is $NiHis_6$, and that this species has extra coordinating atoms on histidine available to form dimers or higher multimers with Ni ions on another His_6. Upon increasing the dose of Ni^{2+} to 2.0, the gels become weaker; this suggests that a different complex species appears, most likely Ni_2His_6, which has no more free histidine so that it does not form any bimolecular complexes.

To understand the data on a more quantitative level, we can make a comparison with low-temperature TR_nT gels, both in terms of frequency dependence and in terms of high-frequency plateau storage modulus. It has been established in previous work [8, 10] that the mechanical properties of TR_nT gels can be quantitatively modelled in terms of a network with a temperature-dependent concentration of exactly trifunctional nodes, which are of course the triple helices T_3. The functionality of the $NiHis_6$ associations is not known *a priori*; solution studies suggest a predominance of dimers $(NiHis_6)_2$, but higher order associations $(NiHis_6)_n$, with n > 2 cannot be excluded. A simple picture would arise if all $NiHis_6$ groups would form dimers; such dimers would be equivalent to TR_4R_4T = TR_8T molecules and therefore one would expect to obtain, at a given TR_4H concentration c, a network equivalent to that of TR_8T at a concentration $c/2$. In order to make the comparison, we have included, in fig. 5A (blue), data from Teles et al.,[10] for G' (high frequency plateau) as a function of

protein concentration for TR_8T networks. The G'(*c*) curve for the Ni/TR_4H gel is indeed rather similar to that of TR_8T, but shifted to higher concentrations. The shift factor, however, is not equal to 2, but somewhat lower (at G'= 500 Pa it is approximately 1.5) indicating that the concentration of nodes in the Ni/TR_4H gel is about 30% higher than expected on the basis of dimerization. This can only be caused by a higher functionality of the $NiHis_6$ connections. The next most likely species is a trimer $(NiHis_6)_3$; hence, we conclude that, most likely, 30 % of the $NiHis_6$ complexes is engaged in a trimer, and the rest in a dimer $(NiHis_6)_2$.

The frequency dependence of the NiTR_4H gel is rather different from that of TR_nT gels: the latter remain elastic up to much longer times. The relaxation times of TR_8T gels in the concentration range 0.5 – 1.0 mM increases from 5000 to 8000 seconds [10], whereas in the present study we found relaxation times for TR_4H which are typically two orders of magnitude lower. This implies that the $NiHis_6$ complexes dissociate much faster than the T_3 triple helices, thereby dominating the relaxation behaviour of the NiTR_4H network.

Conclusions

We have studied self-assembled gels formed by an asymmetric triblock polypeptide TR_4H, where R_4 is a water soluble random coil block, T a triple helix-forming $(PPG)_9$ block, and H stands for a histidine hexamer which is capable of forming complexes with Ni^{2+}. This molecule forms reversible double-trigger ('hybrid') hydrogels when at room temperature and below, and in the presence of Ni^{2+}. The optimum Ni^{2+} dose is between 1:2 and 1:1 (Ni:TR_4H) stoichiometry; at higher dose the gels become weaker, probably because Ni_2His_6 complexes, which cannot bridge to similar complexes, become the dominant species.

The structure of these hydrogels is a polymer network with reversible T_3 triple helices and $NiHis_6$ complexes as connection points and a structure comparable to that of the symmetric

network former TR_8T. On the basis of the high-frequency plateau storage modulus, the $NiHis_6$ complexes are concluded to exist as a mixture of dimers $(NiHis_6)_2$ and trimers $(NiHis_6)_3$. The hybrid gel has a relaxation time of approximately 50 seconds, due to the dynamic nature of the $NiHis_6$ complex; for TR_8T hydrogels in which the reversible histidine-Ni link is replaced by a covalent bond, and relaxation relaxation can only occur through dissociation of triple helices, this is about a hundred times more slowly.

Acknowledgment

MACS acknowledges financial support from ERC Advanced Grant 267254 'BioMate'. We would like to thank Hande Cingil, Gosia Bohdan, Dr. Wolf Rombouts and Remco Fokkink for help with microrheology, metal coordination, rheology, and dynamic light scattering, respectively.

References

1. M. Lemmers, J. Sprakel, I. K. Voets, J. van der Gucht and M. A. Cohen Stuart, *Angew. Chem. Int. Ed.*, 2010, **49**, 708–711.
2. M. Lemmers, E. Spruijt, L. Beun, R. Fokkink, F. Leermakers, G. Portale, M. A. Cohen Stuart and J. van der Gucht, *Soft Matter*, 2012, **8**, 104-117.
3. A. Klymenko, E. Nicol, T. Nicolai and O. Colombani, *Macromolecules*, 2015, **48**, 8169–8176.
4. N. S. Nikouei, N. Ghasemi and A. Lavasanifar, *Pharm. Res.*, 2016, **33**, 358-366.
5. Z. Xu, Y. Liu, S. Guo, S. Jie and B.-G. Li, *J. Appl. Poly, Sci.* , 2016, **133**.
6. J. Sprakel, E. Spruijt, M. A. Cohen Stuart, N. A. M. Besseling, M. P. Lettinga and J. van der Gucht, *Soft Matter*, 2008, **4**, 1696-1705.
7. J. Sprakel, E. Spruijt, M. A. Cohen Stuart, M. A. J. Michels and J. van der Gucht, *Phys. Rev. E*, 2009, **79**, art.no 056306.

8. P. J. Skrzeszewska, F. A. de Wolf, M. W. T. Werten, A. P. H. A. Moers, M. A. Cohen Stuart and J. van der Gucht, *Soft Matter*, 2009, **5**, 2057-2062.

9. P. J. Skrzeszewska, F. A. de Wolf, M. A. Cohen Stuart and J. van der Gucht, *Soft Matter*, 2010, **6**, 416-442.

10. H. Teles, P. J. Skrzeszewska, M. W. T. v. d. G. Werten, Jasper, G. Eggink and F. A. de Wolf, *Soft Matter*, 2010, **6**, 4681-4687.

11. T. T. H. Pham, F. A. de Wolf, M. A. Cohen Stuart and J. van der Gucht, *Soft Matter*, 2013, **9**, 8737-8744.

12. A. Kumar, C. P. Lowe, M. A. Cohen Stuart and P. G. Bolhuis, *Soft Matter*, 2015, **DOI: 10.1039/C5SM01453K**.

13. W. C. Yount, H. Juwarker and S. L. Craig, *J. Am. Chem. Soc.*, 2003, **125**, 15302–15303.

14. W. C. Yount, D. M. Loveless and S. L. Craig, *Angew. Chem.* , 2005, **117**, 2806–2808.

15. D. Xu, C. Liu and S. L. Craig, *Macromolecules*, 2011, **44**, 2343–2353.

16. A. L. Lewis and J. D. Miller, *J. Mater. Chem.*, 1993, **3**, 897-902.

17. A. L. Lewis and J. D. Miller, *J. Mater. Chem.*, 1994, **4**, 729-734.

18. Y. Chujo, K. Sada and T. Saegusa, *Macromolecules* 1993, **26**, 6315–6319.

19. Y. Chujo, K. Sada and T. Saegusa, *Polym. J.*, 1993, **25**, 599-608.

20. C. Wang, R. J. Stewart and J. Kopecek, *Nature* 1999, **397**, 417-420.

21. M. W. T. Werten, H. Teles, A. P. H. A. Moers, E. J. H. Wolbert, J. Sprakel, G. Eggink and F. A. de Wolf, *Biomacromolecules*, 2009, **10**, 1106–1113.

22. L. E. Valenti, C. P. De Pauli and C. E. Giacomelli, *J. Inorg. Biochem.* , 2006 **100**, 192–200.

23. D. E. Fullenkamp, L. He, D. G. Barrett, W. R. Burghardt and P. B. Messersmith, *Macromolecules* 2013, **46**, 1167−1174.

24. Z. Birkó, F. Schauwecker, F. Pfennig, F. Szeszák, S. Vitális, U. Keller and S. Biró, *Fems Microbiol. Lett.* , 2001, **196**, 223-227.

25. A. M. Noubhani, W. Dieryck, S. Chevalier and X. Santarelli, *J. Chromatogr. A* 2002, **968**, 113-120.

26. T. T. H. Pham, J. Wang, M. W. T. Werten, F. Snijkers, F. A. de Wolf, M. A. Cohen Stuart and J. van der Gucht, *Soft Matter*, 2013, **9**, 8923-8930.

27. H. E. Cingil, W. H. Rombouts, J. van der Gucht, M. A. Cohen Stuart and J. Sprakel, *Biomacromolecules*, 2015, **16**, 304–310.

28. J. van der Gucht, N. A. M. Besseling, W. Knoben, L. Bouteiller and M. A. Cohen Stuart, *Phys. Rev. E*, 2003, **67,** , art no 051106.